Research Article

Analysis on Dynamic Response Characteristics of High-Speed Solenoid Valve for Electronic Control Fuel Injection System

Jianyu Zhang,[1,2] **Peng Liu** [iD],[3,4] **Liyun Fan** [iD],[5] **and Yajie Deng**[3,4]

[1]*The 713 Research Institute of CSIC, Zhengzhou 450015, China*
[2]*The Underwater Intelligent Equipment Laboratory of Henan Province, Zhengzhou 450015, China*
[3]*College of Automotive and Mechanical Engineering, Changsha University of Science and Technology, Changsha 410114, China*
[4]*Hunan Provincial Key Laboratory of Intelligent Manufacturing Technology for High-Performance Mechanical Equipment, Changsha University of Science and Technology, Changsha 410114, China*
[5]*College of Power and Energy Engineering, Harbin Engineering University, Harbin 150001, China*

Correspondence should be addressed to Peng Liu; hrbdllp@163.com

A 3D numerical simulation model of high-speed solenoid valve (HSV) for electronic control fuel injection system (ECFIS) has been developed. The model has been validated experimentally with acceptable maximum errors of 2% and 8.7% in closure response time and open response time, respectively. Effect of assembly parameters such as residual air gap, maximum lift of valve stem, mass of the moving parts, spring stiffness, and spring pretightening force on dynamic response characteristics of HSV has been analyzed in detail using the simulation model, and influence rules of various parameters on dynamic response characteristics have been established. Moreover, the correlation between interaction factors of main influence factors and dynamic response characteristics of HSV has also been analyzed. It is concluded that residual air gap, maximum lift of the valve stem, and spring pretightening force are the main influencing factors on dynamic response characteristics of HSV, and there are obvious interaction effects between them; when two or three of these main influencing factors are adjusted at the same time, the interaction effects should be considered.

1. Introduction

With the continuous development of electronic control technology for diesel engines, the electronic control fuel injection system has become an inevitable trend to meet the requirements of increasingly stringent diesel emission regulations [1–4]. HSV is the most widely used automatic control component in ECFIS for diesel. Its dynamic response characteristics directly affect the control precision of the quantity and timing of fuel injection. Fluctuations in the quantity and timing of fuel injection greatly affect the combustion process in the cylinder of diesel engine in terms of economy, power, and emission performance of diesel engine. Therefore, research in the field of dynamic response characteristics of HSV is of significant importance for ECFIS.

At present, there are lots of research materials available regarding this subject mostly focusing on the modeling,

magnetic circuit optimization, and control method of HSV. Melgoza and Rodger [5] developed two new kinds of table models of electromagnetic energy conversion devices with one electrical and one mechanical degrees of freedom and performed a closing transient simulation whose results compared well against measurements. Li and Lee [6] presented an adaptive meshless method for magnetic field computation of an actuator, and it offered a technique to estimate the distribution of numerical errors and a scheme that automatically inserts additional nodes to improve computational accuracy and efficiency. Batdorff and Lumkes [7] introduced a high-fidelity magnetic equivalent circuit model for an axisymmetric electromagnetic actuator, and it improved the accuracy of conventional magnetic equivalent circuit. Cai et al. [8] optimized the plunger, plunger sleeve, coil, and magnetic ring structure parameters of the submersible electromagnetic actuator based on the magnetic

equivalent circuit method. Yin et al. [9] developed the multiphysical field coupling model of solenoid valve for gasoline direct injection considering the electric, magnetic, and thermal properties employing the finite element method and optimized the armature, core, and coil structure parameters based on the multiobjective-simulated annealing algorithm. In [10, 11], peak and hold current control method for solenoid valve was introduced, and the drive circuit was designed and verified which can improve the dynamic response speed and the reliability and satisfy actual application. Lu et al. [12] investigated different driving circuits and control methods for of solenoid value and applied the preenergizing and reverse-energizing control strategy to speed up the response of the solenoid value.

However, very limited research is available on the key assembly parameters of dynamic response characteristics of HSV. These parameters include residual air gap, maximum lift of valve stem, the mass of the moving parts, spring stiffness, and spring pretightening force, which are closely related to the motion state of HSV. Moreover, detailed analysis of interaction effects between different system factors and their influence on dynamic response characteristics of HSV still required to be investigated thoroughly. Interaction effects between different system factors can be understood using Figure 1 as an example. In Figure 1, A and B stand for the individual factors, A * B stands for the interaction factor between A and B, and A * A and B * B stand for the interaction factors with itself. It shows impact of two independent variables A and B on the dependent variable Y. Not only the individual factor A and B will affect Y but also the interaction factors A * B, A * A, and B * B may affect Y because it is a common phenomenon that the factors promote or restrain each other. As a result, the influence degree of other relative variables on the dependent variable will change when a variable is at different levels. Therefore, it is necessary to further study the influences of interaction effect between parameters on dynamic response characteristics of HSV. In this research work, we have used the numerical simulations along with lab experiments to analyze in detail the influence of assembly parameters on dynamic response characteristics of HSV. Key influential assembly parameters have been determined, and the interaction effects between them are studied by the correlation analysis method combined with design of experiments. Research work carried out in this paper decisively provides some theoretical guidance for the selection of parameters and optimal match of HSV.

2. Structures and Work Principle of HSV

This paper focuses on HSV of electronic unit pump (EUP) shown in Figure 2. EUP mainly includes HSV, pump body, plunger, and its reset spring. HSV mainly includes armature, iron core, coil, valve stem, reset spring, terminal, and plug. After turning the power on, iron core attracts armature, pulls the valve stem, closes the seal cone, cuts off fuel, loop and thus sets up high pressure in the pump chamber which is required for fuel injection, whereas turning power off resets all. Resetting spring forces armature to reset the valve stem, decreasing the high-pressure fuel inside the pump chamber
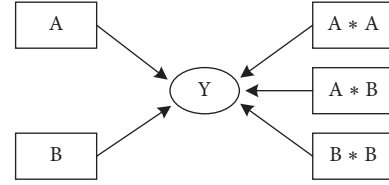

FIGURE 1: Relational graph of two-factor influence.

and thus stopping the fuel injection. Controlling of injection timing and injection quantity can be achieved through precisely adjusting the closing time and duration of control valve stem [13].

3. Methodology

The entire process and method of dynamic response characteristics of HSV are shown in Figure 3. Firstly, the transient numerical model of HSV was developed and validated. Secondly, the parametric influence on dynamic response characteristics of HSV were analyzed using the numerical model, and the key influential assembly parameters were obtained. Thirdly, design of experiments (DOE) was carried out to get sample points, and the response values of sample points were obtained by simulation. Then the correlation coefficients of interaction effect factors were computed. Finally, the correlation analysis was carried out.

3.1. Numerical Modeling

3.1.1. Mathematical Model. Bulleted Maxwell equations for low frequency transient magnetic field can be simplified as follows:

$$\begin{cases} \nabla \times H = \sigma E, \\ \nabla \times E = \dfrac{\partial B}{\partial t}, \\ \nabla \cdot B = 0, \end{cases} \quad (1)$$

where H is the magnetic field, σ is the conductivity of material, E is the electric field intensity, B is the magnetic induction intensity, and t is the time.

The electromagnetic force is computed by the virtual work method:

$$F_{\text{mag}} = \frac{dW(s, i)}{ds}, \quad (2)$$

where F_{mag} is the electromagnetic force on the armature in the direction of the displacement, $W(s,i)$ is the magnetic coenergy of the system, s is the virtual displacement of the armature, and i is the current of coil. $W(s,i)$ is given by

$$W(s, i) = \int_{V} \left(\int_{0}^{H} B \cdot dH \right) dV, \quad (3)$$

where V is the virtually distorted empty area around the armature.

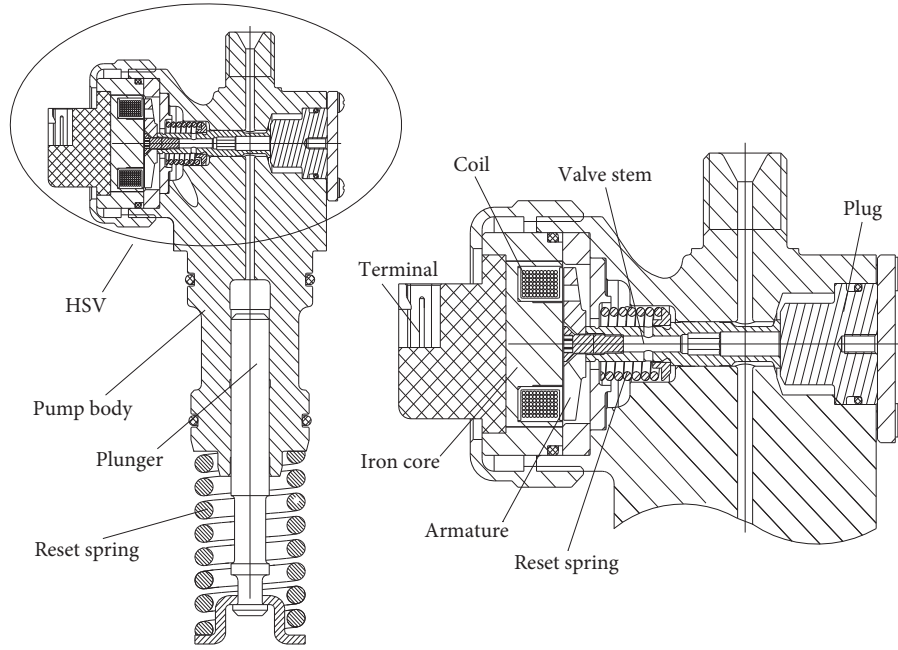After combining equation (2) with equation (3), we get

FIGURE 2: Schematic of EUP and HSV.

$$F_{\text{mag}} = \frac{\partial}{\partial s}\left[\int_V\left(\int_0^H B \cdot \mathrm{d}H\right)\mathrm{d}V\right].\tag{4}$$

The motion equation of the armature is as follows:

$$m\frac{\mathrm{d}^2 x}{\mathrm{d}t^2} = F_{\text{mag}} - \lambda\frac{\mathrm{d}x}{\mathrm{d}t} - kx - F,\tag{5}$$

where m is the mass of the moving parts, x is the displacement, λ is the damping coefficient of movement, k is the spring stiffness, and F is the spring pretightening.

3.1.2. Numerical Modeling in Ansoft Maxwell. The above mathematical model is solved by the finite element method in the software Ansoft Maxwell. HSV is the nonaxisymmetrical structure; therefore, the 3D model has been developed to get the high-precision results, and eddy current has been considered in the Ansoft Maxwell environment. The iron core model is shown in Figure 4(a). It is made of silicon steel sheets with a lamination coefficient of 0.95. The B-H curve of iron core material is shown in Figure 5. The coil model is shown in Figure 4(b). It is combination of a number of copper coils to build into a coil ring. The longitudinal section of the ring is made for the input terminals of excitation. The excitation type is set to current, and the measured currents are imported as excitation. The armature model is shown in Figure 4(c) whose material is DT4 (electrician pure iron). Since the moving parts in the Ansoft Maxwell modeling environment must be a three-dimensional entity and have a real boundary, the surfaces of moving parts cannot be curved surfaces but a divisible plane. To meet the requirements, an extra polygon cylinder surrounding the armature is built, and its material is set to air. Besides, a moving region was built to separate the static parts from the moving parts. Finally to
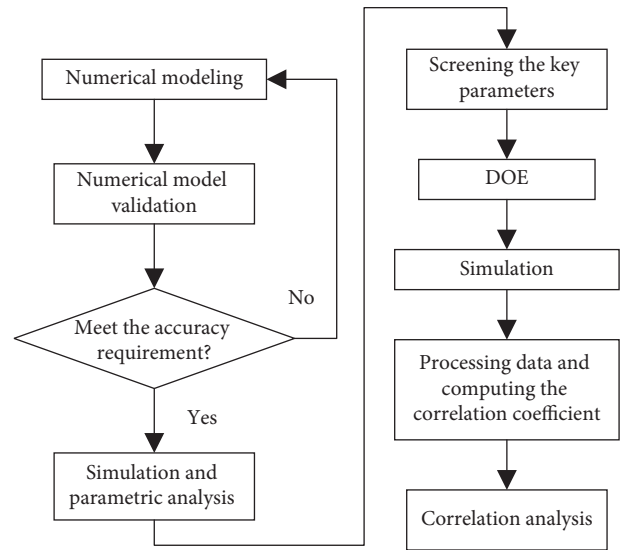

FIGURE 3: Research flowchart.

make magnetic field boundary conditions satisfy the infinite far field boundary conditions, the solution domain was established to surround the entire model with air. The whole model including the solution domain is shown in Figure 4(d).

3.2. Numerical Model Validation. Figure 6 shows the test bench for dynamic response of HSV. It consists of EUP, HSV, control unit, oscilloscope, eddy current displacement sensor, and current probe. The eddy current displacement sensor is placed suitably at the plug of EUP to measure the displacement of the valve stem. Coil current of HSV is
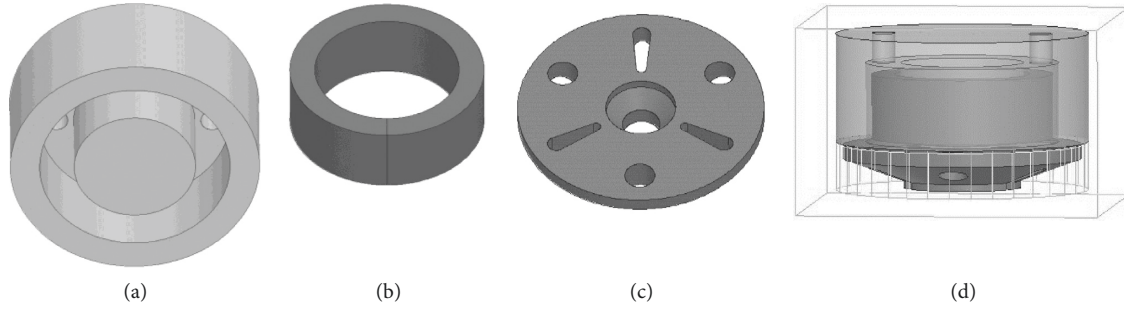
FIGURE 4: Ansoft simulation model of HSV: (a) Iron core model. (b) Coil model. (c) Armature model. (d) The whole model.
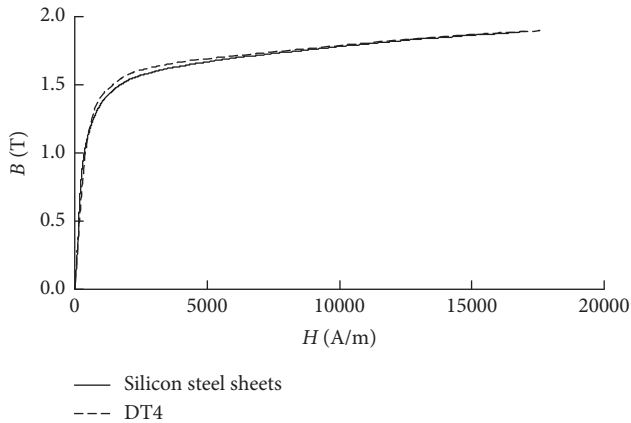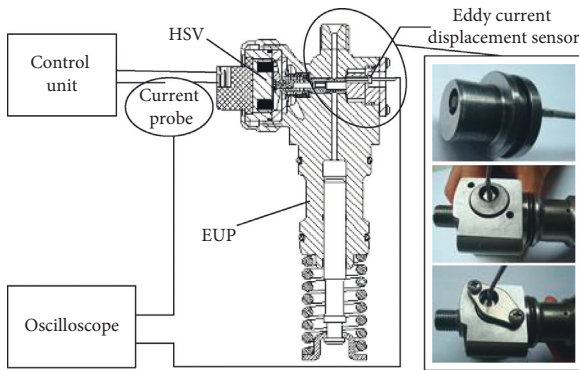

FIGURE 5: B-H curves of materials.

FIGURE 6: Test bench for dynamic response of HSV.

measured in real time by using the current probe and transferred to the oscilloscope. The multiple groups of experimental results at the typical working conditions have been obtained by changing the cam rotational speeds and injection pulse widths to the controller.

The evaluation index of dynamic response of HSV includes the closure response time t_c and the open response time t_o (as shown in Figure 7). We imported the measured currents at the typical working conditions to the numerical model as excitation, respectively, and carried out simulations to get the simulated results. Table 1 shows comparisons between the simulated and experimental results.

According to Table 1, the maximum error of the closure response time of HSV is 2%. Moreover, the simulated results of the closure response time are all less than the experimental result. Two reasons for less simulated closure times are because we have ignored the friction in the movement of armature and also not considered the rising of the temperature of the solenoid valve which can lead to the decrease in the magnetic permeability of armature and iron core. The maximum error of the open response time of HSV is 8.7%, and the simulated results of the open response time are also all less than the experimental result. The reason for less open simulation response time is that the initial magnetization curve was employed to describe the entire process of magnetization in simulation, which ignored the hysteresis effect. In fact, the hysteresis loop of soft magnetic material is very narrow. So we can use the initial magnetization curve to describe the entire process of magnetization. The error in simulations is considered within acceptable range when comparing with experiments, therefore validating the numerical model of HSV for next research on dynamic response of HSV.

3.3. DOE.
DOE is a technology which is used widely, and central composite design (CCD) is one of the most popular DOEs. It can efficiently and reliably provide sample points for computing the correlation coefficients. CCD is a mixture of the traditional interpolation node distribution mode and full-factor or partial-factor design, which can provide more information with as little experiments as possible, including variable effects and test error [14]. Its design points consist of 2^n factorial design points or partial-factor design points, $2n$ axial points or star points, and n_c center points. Figure 8 shows the CCD of two factors in which n is 2. The distances are ± 1 between center points and high or low level of factors (variables in standardized units). The distances are $\pm \alpha$ between center points and axial points or star points. It is called central composite face (CCF) when α takes 1 [15]. CCF has been used in this paper.

3.4. Correlation Analysis.
Correlation analysis refers to two or more factors. The purpose is to measure how closely their correlativity between two factors is. Correlation coefficient R represented by equation (6) is a quantitative indicator for studying the degree of linear correlation between two
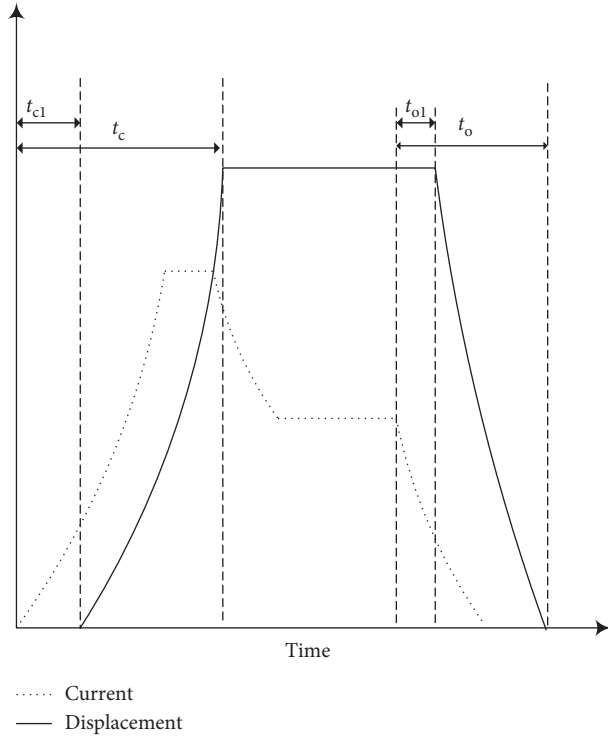
Figure 7: Schematic of the response time of HSV.

Table 1: Comparison of simulation and experiment.

Typical working conditions		Simulation		Experiment		Error (%)	
Cam rotational speeds (r/min)	Injection pulse widths (°CaA)	t_c (ms)	t_o (ms)	t_c (ms)	t_o (ms)	t_c	t_o
975	3.8	0.658	0.496	0.668	0.543	1.5	8.7
1200	2.1	0.694	0.524	0.698	0.55	0.6	4.7
1200	4.2	0.698	0.520	0.7	0.555	0.3	6.3
1425	4.8	0.72	0.544	0.735	0.593	2.0	8.3

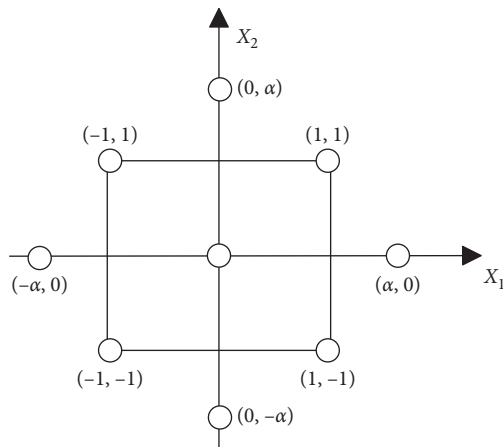CaA stands for the rotation angle of the cam.

Figure 8: CCD of two factors.

factors. In equation (6), x is the studied factor, y is the corresponding response valve, i is the number i design sample point, n is the total number of sample points of DOE, $\overline{x}$ is the average of this factor, and $\overline{y}$ is the average of this response. The range of correlation coefficient R is from -1 to 1. R more than zero shows a positive correlation between two factors, whereas R less than zero shows a negative correlation between two factors. The larger the absolute value of correlation coefficient R is, the closer the correlation between the two factors is:

$$R = \frac{\sum_{i=1}^{n} (x_i - \overline{x})(y_i - \overline{y})}{\sqrt{\sum_{i=1}^{n} (x_i - \overline{x})^2 \sum_{i=1}^{n} (y_i - \overline{y})^2}}. \tag{6}$$

4. Results and Analysis

4.1. Individual Assembly Factor Analysis. The main assembly parameters of HSV includes residual air gap, maximum lift of the valve stem, the mass of the moving parts, spring stiffness, and spring pre-tightening force. Table 2 shows the studied range of every parameter. In this paper, the measured current at 1200 r/min cam rotational speed with 7.2°CaA injection pulse width was imported to the numerical model as excitation to research the dynamic response of HSV. All other parameters have been considered with their reference values when carrying out single parameter analysis.

4.1.1. Residual Air Gap. Residual air gap is the distance from iron core to armature after HSV closure. It has an obvious influence on the dynamic response of HSV as shown in Figure 9. With the increase of residual air gap from 0.04 mm to 0.12 mm, actuation trigger time (t_{c1} as shown in Figure 7) increases from 0.114 ms to 0.156 ms, and the closure response time of HSV increases from 0.478 ms to 0.602 ms; release trigger time (t_{o1} as shown in Figure 7) decreases from 0.126 ms to 0.056 ms, and the open response time of HSV decreases from 0.584 ms to 0.486 ms because the working air gap of HSV consists of residual air gap and valve stem lift. So the increase of residual air gap makes the increase of working air gap, when keeping the valve stem lift unchanged. It leads to the increase of magnetic resistance, and as a result, the electromagnetic force decreases. Consequently, the actuation trigger time and the closure response time of HSV increase. However, for the opening process of HSV, electromagnetic force is resistance. Therefore release trigger time and the open response time of HSV decrease. When comparing the change of release trigger time with the open response time of HSV, it can be found that residual air gap affects the open response time of HSV by release trigger time. Besides, residual air gap makes a greater influence on the closure response time than the open response time. Therefore, a smaller residual air gap is suggested with two potential benefits. Firstly, it can improve the whole response speed of HSV. Secondly, the hold current can be reduced after the HSV closes, which can reduce the power loss and heat production of the coil.

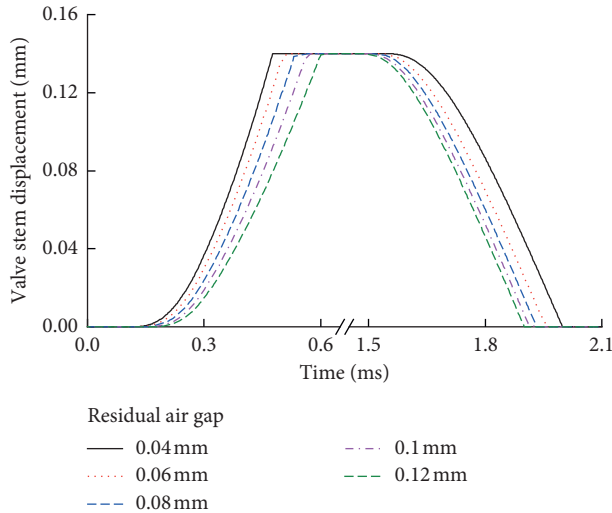| Factors	Reference value	Range
Residual air gap, d (mm)	0.08	0.04–0.12
Maximum lift of valve stem, S (mm)	0.14	0.1–0.18
Mass of the moving parts, m (g)	12	8–16
Spring stiffness, k (N/mm)	14	6–22
Spring pretightening, F (N)	60	50–70

Residual air gap

— 0.04 mm   –·– 0.1 mm
···· 0.06 mm   ––– 0.12 mm
––– 0.08 mm

FIGURE 9: Influence of residual air gap on the dynamic response of HSV.

Maximum lift of valve stem

— 0.1 mm   –·– 0.16 mm
···· 0.12 mm   ––– 0.18 mm
––– 0.14 mm

FIGURE 10: Influence of maximum lift of the valve stem on the dynamic response of HSV.

4.1.2. Maximum Lift of Valve Stem. Just like residual air gap, the maximum lift of the valve stem also has an obvious influence on the dynamic response of HSV as shown in Figure 10. With the increase of maximum lift of the valve stem from 0.1 mm to 0.18 mm, actuation trigger time increases from 0.114 ms to 0.156 ms, and the closure response time increases from 0.418 ms to 0.676 ms; release trigger time keeps unchanged, and the open response time of HSV decreases from 0.434 ms to 0.598 ms. Movement distance of armature increases with the increase of maximum lift of the valve stem. Moreover, by keeping the residual air gap unchanged, increase of the maximum lift of the valve stem increases the initial working air gap too. This leads to an increase of magnetic resistance and decrease of electromagnetic force. As a result, actuation trigger time and the closure response time of HSV increase. By keeping residual air gap and drive current unchanged, the increase of the movement distance obviously leads to the increase of the open response time of HSV. Therefore, decreasing the maximum lift of the valve stem can effectively improve the response speed of HSV. But sudden and quick discharge of high pressure oil can be a problem with less available drainage area. Therefore, it is recommended that the maximum lift of the valve stem should be considered wisely.

4.1.3. Mass of the Moving Parts. Effect of mass of the moving parts on the dynamic response of HSV is shown in Figure 11.
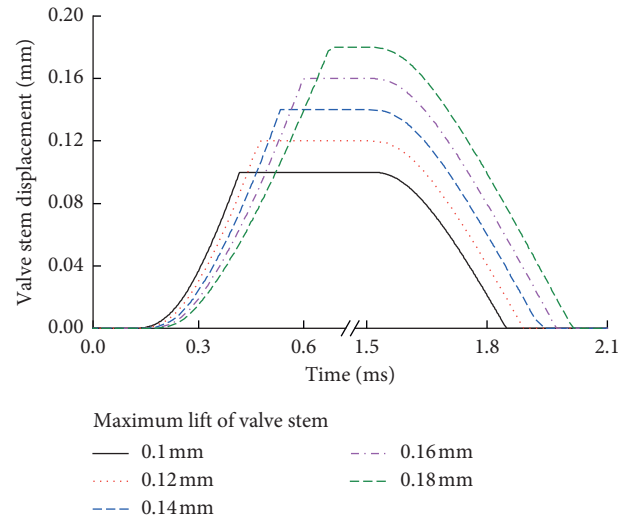
It mainly impacts on both the whole closure response and open response time and slightly on the actuation trigger time and release trigger time. With the increase of mass of the moving parts from 8 g to 16 g, the closure response time and open response time increase from 0.5 ms to 0.566 ms and 0.484 ms to 0.544 ms, respectively. The increase of mass of the moving parts inevitably decreases the acceleration of armature, resulting in the increase of response time. Therefore, mass of the moving parts should be designed as light as possible where it meets the structure strength requirements. In the armature processing, generally a groove or a hole can be made in armature at appropriate location. This can weaken the effect of vortex and reduces the mass of the moving parts.

4.1.4. Spring Stiffness. Spring stiffness has little influence on the dynamic response of HSV as shown in Figure 12. Because valve stem lift is only 0.16 mm, even with the different values of stiffness, the deformation force is too small as compared to the pretightening and electromagnetic force.

4.1.5. Spring Pretightening. Spring pretightening also has a defined impact on the dynamic response of HSV as shown in Figure 13. With the increase of pretightening from 50 N to 70 N, both actuation trigger time and closure response time increase from 0.12 ms to 0.15 ms and 0.492 ms to 0.592 ms, respectively, whereas release trigger time and open response time decrease from 0.1 ms to 0.068 ms and 0.586 ms to 0.466 ms, respectively. In fact, the bigger the pretightening is, the faster the closure response time changes, and the slower the open response time changes because spring force almost keeps unchanged during the movement process of armature with small valve stem lift. Therefore, pretightening is the main resistance during the closing process of HSV. Any increase in pretightening will increase current required to move armature, and as a result, the actuation
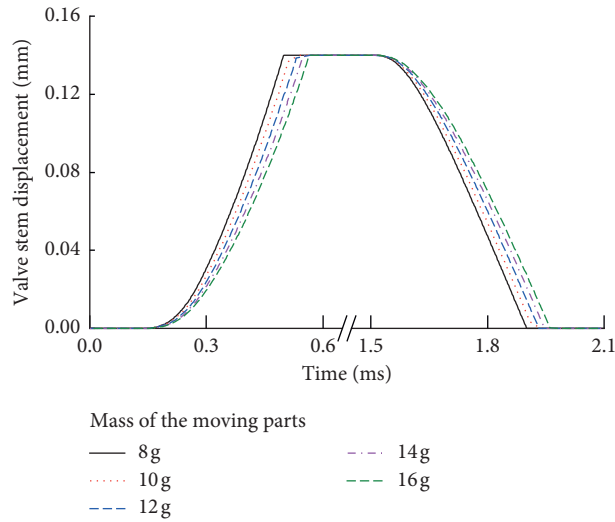
FIGURE 11: Influence of mass of the moving parts on the dynamic response of HSV.
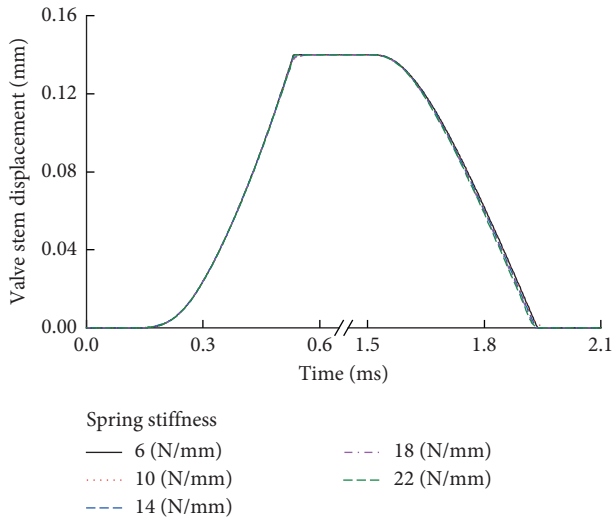

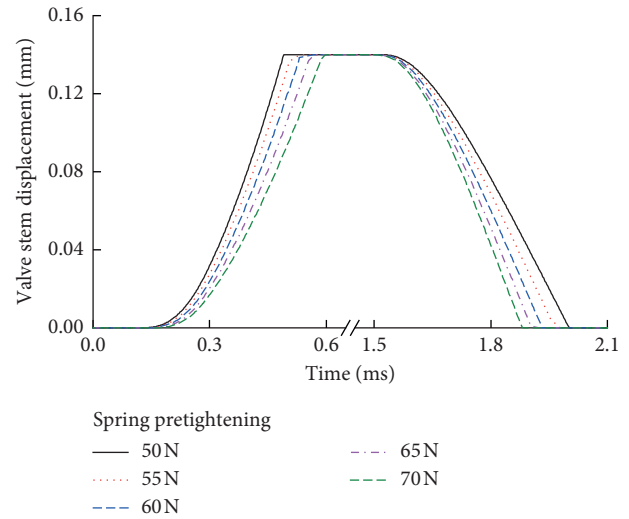FIGURE 12: Influence of spring stiffness on the dynamic response of HSV.

FIGURE 13: Influence of spring pretightening on the dynamic response of HSV.

trigger time increases. Moreover acceleration of armature also decreases with the increase of pretightening, thereby increasing the closure response time of HSV. On the contrary, pretightening is the main driving force during the opening process of HSV; therefore, the release trigger time and open response time of HSV decrease with the increase of spring pretightening. So when it meets the requirement of the open response time of HSV, it should use a smaller pretightening.

4.2. Correlation Analysis. We have concluded after individual assembly factor analysis that spring stiffness has little influence on dynamic response characteristics of HSV; therefore, the interaction effect has been analyzed between remaining four factors only. Twenty-seven experimental points were designed by CCF, and their response values were

obtained by the simulation model as shown in Table 3. Correlation coefficients between all factors and the response time of HSV were obtained using equation (6) and are shown in Figure 14.

Correlation coefficients of the second-order factors of parameter self-interaction ($d * d$, $S * S$, $m * m$, and $F * F$) are almost similar and are around 0.1 as shown in Figure 14. It shows that the factors of parameter self-interaction have little influence on dynamic response characteristics of HSV. Correlation coefficients of interactions between two different parameters including residual gas gap with maximum lift of valve stem ($d * S$), residual gas gap with spring pretightening force ($d * F$), and maximum lift of the valve stem with spring pretightening force ($S * F$) are the main influential factors. Their correlation coefficients are 0.17, 0.14, and 0.18, respectively, for the closure response time, and 0.13, 0.13, and 0.09, respectively, for the total response

TABLE 3: Experimental design scheme and results.

| Number	d (mm)	S (mm)	m (g)	F (N)	t_c (ms)	t_o (ms)	t (ms)
1	0.04	0.1	8	50	0.322	0.532	0.854
2	0.04	0.1	8	70	0.37	0.42	0.79
3	0.04	0.1	16	50	0.372	0.596	0.968
4	0.04	0.1	16	70	0.426	0.478	0.904
5	0.12	0.1	8	50	0.402	0.424	0.826
6	0.12	0.1	8	70	0.48	0.334	0.814
7	0.12	0.1	16	50	0.456	0.482	0.938
8	0.12	0.1	16	70	0.544	0.388	0.932
9	0.04	0.18	8	50	0.508	0.724	1.232
10	0.04	0.18	8	70	0.618	0.56	1.178
11	0.04	0.18	16	50	0.578	0.796	1.374
12	0.04	0.18	16	70	0.702	0.626	1.328
13	0.12	0.18	8	50	0.638	0.616	1.254
14	0.12	0.18	8	70	0.926	0.474	1.4
15	0.12	0.18	16	50	0.722	0.68	1.402
16	0.12	0.18	16	70	1.064	0.536	1.6
17	0.08	0.14	12	50	0.492	0.586	1.078
18	0.08	0.14	12	70	0.592	0.466	1.058
19	0.08	0.14	8	60	0.5	0.486	0.986
20	0.08	0.14	16	60	0.566	0.546	1.112
21	0.04	0.14	12	60	0.478	0.584	1.062
22	0.12	0.14	12	60	0.602	0.486	1.088
23	0.08	0.1	12	60	0.412	0.434	0.846
24	0.08	0.18	12	60	0.676	0.598	1.274
25	0.08	0.14	12	60	0.534	0.518	1.052
26	0.08	0.14	12	60	0.534	0.518	1.052
27	0.08	0.14	12	60	0.534	0.518	1.052
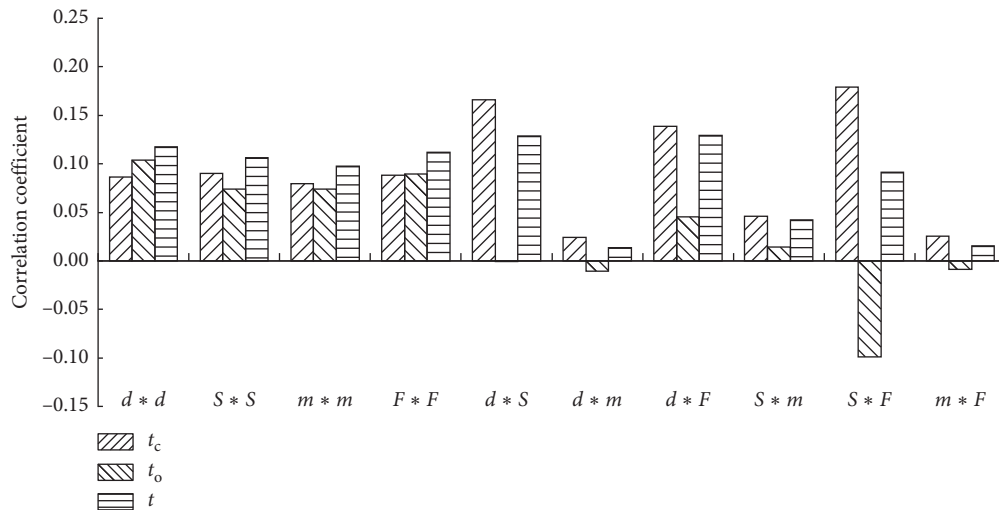
FIGURE 14: Correlation of each factor with response time.

time t. They have relatively great influence on the closure response time and the open response time of HSV. So the interaction effects should be considered and multiparameter optimization strategy is recommended to do it, when two or three of these parameters—residual air gap, maximum lift of valve stem, and spring pretightening force—are adjusted at the same time. Other factors have no obvious correlation with dynamic response characteristics of HSV.

5. Conclusions

(1) A numerical simulation model of HSV has been developed in the Ansoft Maxwell environment, and its accuracy has been validated experimentally. It provides an effective platform for the research on the dynamic response characteristics of HSV.

(2) These assembly parameters—residual air gap, maximum lift of valve stem, and spring pretightening

force—have significant influence on dynamic response characteristics of HSV, and there are obvious interaction effects between these parameters. When two or three of them are adjusted at the same time, the interaction effects should be considered and multiparameter optimization strategy is recommended to do it.

Data Availability

The data used to support the findings of this study are included within the article.

Conflicts of Interest

The authors declare that there are no conflicts of interest regarding the publication of this paper.

Acknowledgments

References

[1] T. Qiu, H. Dai, Y. Lei, C. Cao, and X. Li, "Optimising the cam profile of an electronic unit pump for a heavy-duty diesel engine," *Energy*, vol. 83, pp. 276–283, 2015.

[2] M. R. Herfatmanesh, P. Lu, M. A. Attar et al., "Experimental investigation into the effects of two-stage injection on fuel injection quantity, combustion and emissions in a high-speed optical common rail diesel engine," *Fuel*, vol. 109, pp. 137–147, 2013.

[3] G. A. P. Rao and S. Kaleemuddin, "Development of variable timing fuel injection cam for effective abatement of diesel engine emissions," *Applied Energy*, vol. 88, pp. 2653–2662, 2011.

[4] P. Liu, L. Y. Fan, H. Qaisar et al., "Research on key factors and their interaction effects of electromagnetic force of high-speed solenoid valve," *Scientific World Journal*, vol. 2014, Article ID 567242, 13 pages, 2014.

[5] E. Melgoza and D. Rodger, "Comparison of table models of electromagnetic actuators," *IEEE Transactions on Magnetics*, vol. 38, no. 2, pp. 953–956, 2002.

[6] Q. Li and K.-M. Lee, "An adaptive meshless method for magnetic field computation," *IEEE Transactions on Magnetics*, vol. 42, no. 8, pp. 1996–2003, 2006.

[7] M. A. Batdorff and J. H. Lumkes, "High-fidelity magnetic equivalent circuit model for an axisymmetric electromagnetic actuator," *IEEE Transactions on Magnetics*, vol. 45, no. 8, pp. 3064–3072, 2009.

[8] B. Cai, Y. Liu, A. Abulimiti et al., "Optimal design based on dynamic characteristics and experimental implementation of submersible electromagnetic actuators," *Strojniški Vestnik-Journal of Mechanical Engineering*, vol. 59, pp. 473–482, 2013.

[9] C. Yin, Z. Zhang, Y. Sun, N. Xie, and Q. Cheng, "Optimization of magnetic circuit configuration for GDI injector based on MOSA algorithm," *International Journal of Applied Electromagnetics and Mechanics*, vol. 49, no. 4, pp. 531–546, 2015.

[10] D. Huang, H. Y. Ding, Z. W. Wang et al., "Design of drive circuit for GDI injector," in *Proceedings of the 2011 International Conference on Electric Information and Control Engineering*, pp. 5821–5824, Wuhan, China, April 2011.

[11] W. C. Tsai and P. C. Yu, "Design of the electrical drive for the high-pressure GDI injector in a 500cc motorbike engine," *International Journal of Engineering and Industries*, vol. 2, no. 1, pp. 70–83, 2011.

[12] H. Lu, J. Deng, Z. Hu, Z. Wu, and L. Li, "Impact of control methods on dynamic characteristic of high speed solenoid injectors," *SAE International Journal of Engines*, vol. 7, no. 3, pp. 1155–1164, 2014.

[13] L. Y. Fan, W. Q. Long, Y. X. Zhu et al., "A characteristic study of electronic in-line pump system for diesel engines," in *Proceedings of the SAE Technical Paper*, Detroit, MI, USA, April 2008.

[14] M. Ahmadi, F. Vahabzadeh, B. Bonakdarpour, E. Mofarrah, and M. Mehranian, "Application of the central composite design and response surface methodology to the advanced treatment of olive oil processing wastewater using Fenton's peroxidation," *Journal of Hazardous Materials*, vol. 123, no. 1–3, pp. 187–195, 2005.

[15] E. Rosales, M. A. Sanromán, and M. Pazos, "Application of central composite face-centered design and response surface methodology for the optimization of electro-Fenton decolorization of Azure B dye," *Environmental Science and Pollution Research*, vol. 19, no. 5, pp. 1738–1746, 2012.